Article

Increasing the Performance of a Fiber-Reinforced Concrete for Protective Facilities

Roman Fediuk [1],*[ID], Mugahed Amran [2,3][ID], Sergey Klyuev [4][ID] and Aleksandr Klyuev [4]

1   Polytechnical Institute, Far Eastern Federal University, 690922 Vladivostok, Russia
2   Department of Civil Engineering, College of Engineering, Prince Sattam Bin Abdulaziz University, Alkharj 16273, Saudi Arabia; m.amran@psau.edu.sa
3   Department of Civil Engineering, Faculty of Engineering and IT, Amran University, Amran 9677, Yemen
4   Belgorod State Technological University Named after V.G. Shukhov, 308012 Belgorod, Russia; klyuyev@yandex.ru (S.K.); klyuyevav@yandex.ru (A.K.)
*   Correspondence: roman44@yandex.ru

Abstract: The use of fiber in cement materials is a promising and effective replacement for bar reinforcement. A wide range of fiber-reinforced concretes based on composite binders with increased impact strength characteristics have been developed. The synthesized composites included the composite binder made of Portland cement, silica, and carbonate additives. Basalt and steel were used as fibers. The nature of the influence of the composition and manufacturing technology of cement composites on the dynamic hardening coefficient has been established, while the growth of these indicators is achieved by creating a denser interfacial transition zone between the cement paste, aggregate, and fiber as a result of improving the homogeneity of the concrete mixture and controlling the consistency. Workability indicators (slump flow up to 730 mm; spreading time up to a diameter of 50 cm is up to 3 s) allow them to be classified as self-compacting concrete mixtures. An increase in the values of the impact strength coefficient by a factor of 5.5, the dynamic hardening coefficient by almost 70% as a result of interfacial interaction between fibers and binder matrix in the concrete composite, as well as absorption of impact energy by fiber, was revealed. The formula describing the effect of the loading rate on the coefficient of dynamic hardening of fiber-reinforced concrete has been refined. The fracture processes of the obtained materials have been established: after the initiation of primary cracks, the structure of the composite absorbs impact energy for a long time, while in the inelastic range (the onset of cracking and peak loads), a large number of secondary cracks appear.

Keywords: fiber concrete; cement composite; dynamic strength; impact strength

1. Introduction

The use of fibers as reinforcement is not a new notion. Since ancient times, fibers have been employed as reinforcement [1,2]. Horsehair was once used in straw in mud-bricks and mortar. Asbestos fibers were employed in concrete in the early 1900s. The concept of composite materials was born in the 1950s, and fiber-reinforced concrete was one of the hot issues. There was a need to find a replacement for asbestos in concrete and other building materials after the health dangers linked with the substance were revealed. Steel [3], glass (GFRC) [4], and synthetic (polypropylene) fibers were all employed in concrete by the 1960s. New fiber-reinforced concretes are still being researched [5–7]. Fibers that are overly long and not adequately treated at the time of processing, on the other hand, tend to "ball" in the mix and cause problems with workability [8]. Fibers are added to concrete for long-term durability by controlling the size of cracks, by which the transport of corrosive materials into the concrete is reduced [5,6,8].

Fiber-reinforced building materials for special structures, created taking into account transdisciplinary positions and micromechanics of composite media, are of significant interest as a new generation of composites [5,6,8]. At the same time, it becomes possible to

achieve the target characteristics of static and dynamic strength, impermeability to toxic vapors and gases, as well as durability, which will make it possible to operate structures in extreme conditions and, accordingly, preserve the life and health of people in protective shelters [9–11]. Transdisciplinary positions that combine the theoretical foundations and technical justification for the creation of multicomponent composites from the standpoint of reducing the economic and environmental burden, provide the ability to control structure formation in order to achieve high values of operational characteristics [7–15].

Fibers are commonly used in concrete to prevent cracking caused by shrinkage of the cement paste at the plastic stage, drying and autogenous shrinkage in the early stage [15–17]. Concrete with certain fibers has higher impact, abrasion, and shatter resistance [16]. In some cases, larger steel or synthetic fibers can totally replace rebar or steel [18]. In the underground construction industry, fiber-reinforced concrete has nearly completely replaced bar in tunnel segments, with almost all tunnel linings being fiber-reinforced rather than rebar [19,20]. Some fibers do, in fact, lower concrete's compressive strength [21]. A number of works are devoted to the development of effective methods for the manufacture of structural fiber-reinforced materials for protective structures [22–25]. Li [26] has developed engineering concrete composites that can be effectively applied to earthquake-resistant construction. The mechanical properties of high-strength fiber-reinforced concrete were studied in detail by Yoo [27]. Good results, generalized by Ranjbar [28], were obtained in experiments with geopolymers. A significant effect is provided by the use of secondary aggregate from concrete scrap of demolished buildings and structures [16]. As it was revealed as a result of a literature review [7–15], with the acceleration of loading (and hence deformation), the material acquires dynamic strength. A representative parameter of this kind of hardening is the coefficient of dynamic hardening (*CDH*), which is the ratio of dynamic compressive strength to static one.

CEB-FIP code [29] propose the following formula for calculating the *CDH:*

$$CDH = \frac{f_{cd}}{f_{cs}} = \left(\frac{\dot{\varepsilon}}{\dot{\varepsilon}_s}\right)^{1.026\alpha_s} \text{ at } \dot{\varepsilon} \leq 30 \text{ s}^{-1}$$

$$CDH = \frac{f_{cd}}{f_{cs}} = \gamma_s \left(\frac{\dot{\varepsilon}}{\dot{\varepsilon}_s}\right)^{1/3} \text{ at } \dot{\varepsilon} > 30 \text{ s}^{-1}$$

here f_{cd} is an ultimate strength in dynamic compression; f_{cs} is an ultimate strength in static compression; $\dot{\varepsilon}$ is a strain rate in the range from 3×10^{-5} to 3×10^2 reciprocal seconds (calculated as the strain under axial compression, divided by the time taken to reach this value); $\dot{\varepsilon}_s$ is a strain rate under static compression, equal to 3×10^{-5} reverse seconds;

$$\gamma_s = 10^{(6.156\alpha_s - 2)}$$

$$\alpha_s = \frac{1}{5 + 9 f_{at}/f_{co}}$$

$$f_{co} = 10 \text{ MPa}$$

A known way to increase flexural strength, tensile strength, and impact viscosity is the use of fibers from various materials in cement composites. At the same time, among the various types of fiber, the use of steel and basalt fiber gives good results [15,18,19,21]. At the same time, there is a need for the formation of concepts to supplement the fundamental foundations using models of hydration structure formation of cement composites for various functional purposes [30,31]. Considering that the science intensity of industries is determined, among other things, by the rate of change of raw materials, it is important to expand the raw material base for the creation of new structural materials with various improved target characteristics [32–35]. At the same time, to date, the rate of change of raw materials in the construction industry remains quite low [36–38]. Manufacturers are in no hurry to massively introduce unconventional raw materials due to their unwillingness

to re-equip existing technological lines as well as due to regulations prohibiting many changes [39–43].

Thus, based on a comprehensive analysis of literature sources, it is urgent to develop scientific foundations for managing the processes of synthesis of composites at various scale levels, with the identification of the stages of structure formation of composite binding systems and interaction of the raw materials.

The hypothesis of the work is that a combination of mixed binder with fibers will have a synergetic effect. Therefore, the aim of the article is to measure the composition effect on mechanical behavior. The goal is to develop composite binders and cement fiber concretes with improved dynamic strength. However, the research significance of the study lies in complementing the theoretical foundations for controlling the processes of synthesis of cement composites at various scale levels.

2. Materials and Methods

2.1. Materials

The following raw materials were used:

—   for the composite binder: Portland cement CEM I 42.5N according to EN-197 [44], active silica-containing additive, ground quartz sand, limestone microfiller;
—   for the self-compacting concrete mix: Pantarhit PC 160 superplasticizer, quartz sand, steel, and basalt fiber (Figure 1, Table 1).

| (a) | (b) |

Figure 1. Fibers used: (**a**) steel, (**b**) basalt.

Table 1. Technical characteristics of the types of fibers used.

Characteristics	Steel Fiber	Basalt Fiber
Tensile strength, MPa	600–1500	3500
Fiber diameter, mm	1.2	13×10^{-3}
Fiber length, mm	13	6 ± 1.5
Elastic modulus, GPa	190	75
Elongation ratio, %	3.5	3.2
Melting temperature, °C	1550	1450
Resistant to alkalis and corrosion	medium	high
Density, kg/m^3	7800	2600

One of the active mineral fillers in the composition of the composite binder is the active silica-containing additive (ASCA), which is obtained by the technology of heat treatment of rice husk, which makes it possible to obtain a material with a high content of silicon dioxide (up to 99%); it includes controlled combustion of raw materials for 2 h at a temperature of 900 °C. As a result, silica particles were obtained that did not exceed 60 μm in size (Figure 2).
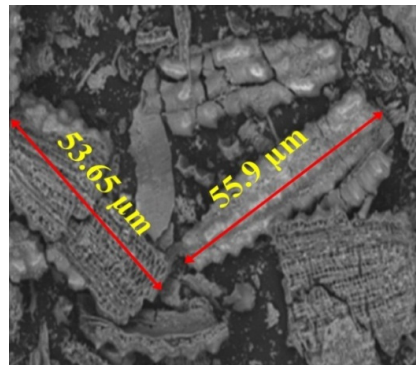
Figure 2. Morphology of the active silica-containing additive.

2.2. Mix Design

The introduction of ASCA as a partial replacement for cement confirms its efficiency up to substitution at the level of about 30%, and this trend remains for the fineness of grinding in the range from 500 to 900 m^2/kg (Figure 3). In this case, the maximum effect is achieved with a specific surface area of 550 m^2/kg; a further increase in the fineness of grinding does not lead to an increase in activity.
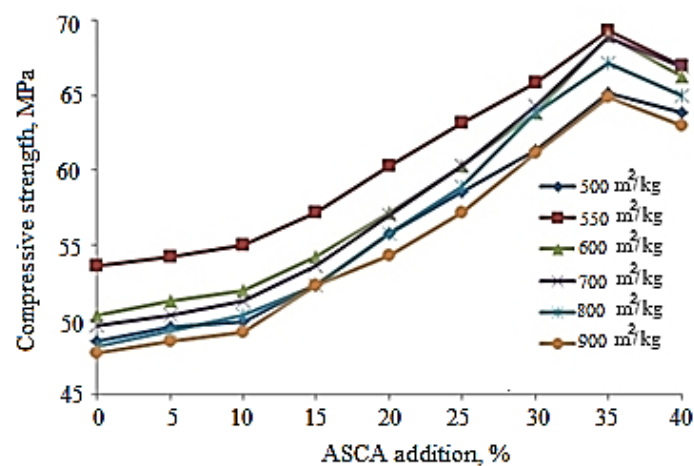

Figure 3. Dependence of the compressive strength of cement paste on the amount of added ASCA.

A wide range of composite binders has been developed (Table 2). Here the reference composition (CEM) was not subjected to grinding, and all other compositions were ground to 550 m/kg.

Table 2. The developed nomenclature of the composite binders.

Mix ID	Properties pf the Binder, %				Superplasticizer, % of the Binder
	Portland Cement	Ground Quartz Sand	Limestone	ASCA	
1-1	70	2.5	2.5	25	1.0
1-2	64	2.5	2.5	31	1.3
1-3	58	2.5	2.5	37	1.6
2-1	65	5	5	25	1.0
2-2	59	5	5	31	1.3
2-3	63	-	-	37	1.6
3-1	60	7.5	7.5	25	1.0
3-2	-	-	-	31	1.3
3-3	63	-	-	37	1.6
CEM	100	-	-	-	-

Based on composite binders, self-compacting fiber-reinforced concretes have been obtained, which have the potential for use in the structures of protective structures. For this, 1020 kg of sand, 235 L of water, and 1.6% volume (of the composite binder) of steel or basalt fiber were added to 1 cubic meter of concrete mix. The water to binder ratio was 0.4.

2.3. Methods

The study of the specific surface area of the components of the composite binder was carried out using a PSH-11 device (Khodakov Devices, Moscow, Russia) (Figure 4a). The microstructure of the raw materials was studied using a scanning electron microscope (CrossBeam 1540XB, Berlin, Germany) (Figure 4b). X-ray diffraction analysis was carried out on an equipment ARL 9900 WORKSTATION (Thermo Fisher Scientific, Waltham, MA, USA) (Figure 4c). The study of the normal density of the mixtures according to the Russian Standard GOST 310.3-76 was carried out on a rotational viscometer RheoStress 600 (HAAKE, Berlin, Germany) with a measuring system FL22 (propeller type), shown in Figure 4d. The consistency of the cement paste was taken as the normal consistency, in which the pestle does not reach the bottom of the measuring container by 5–7 mm.
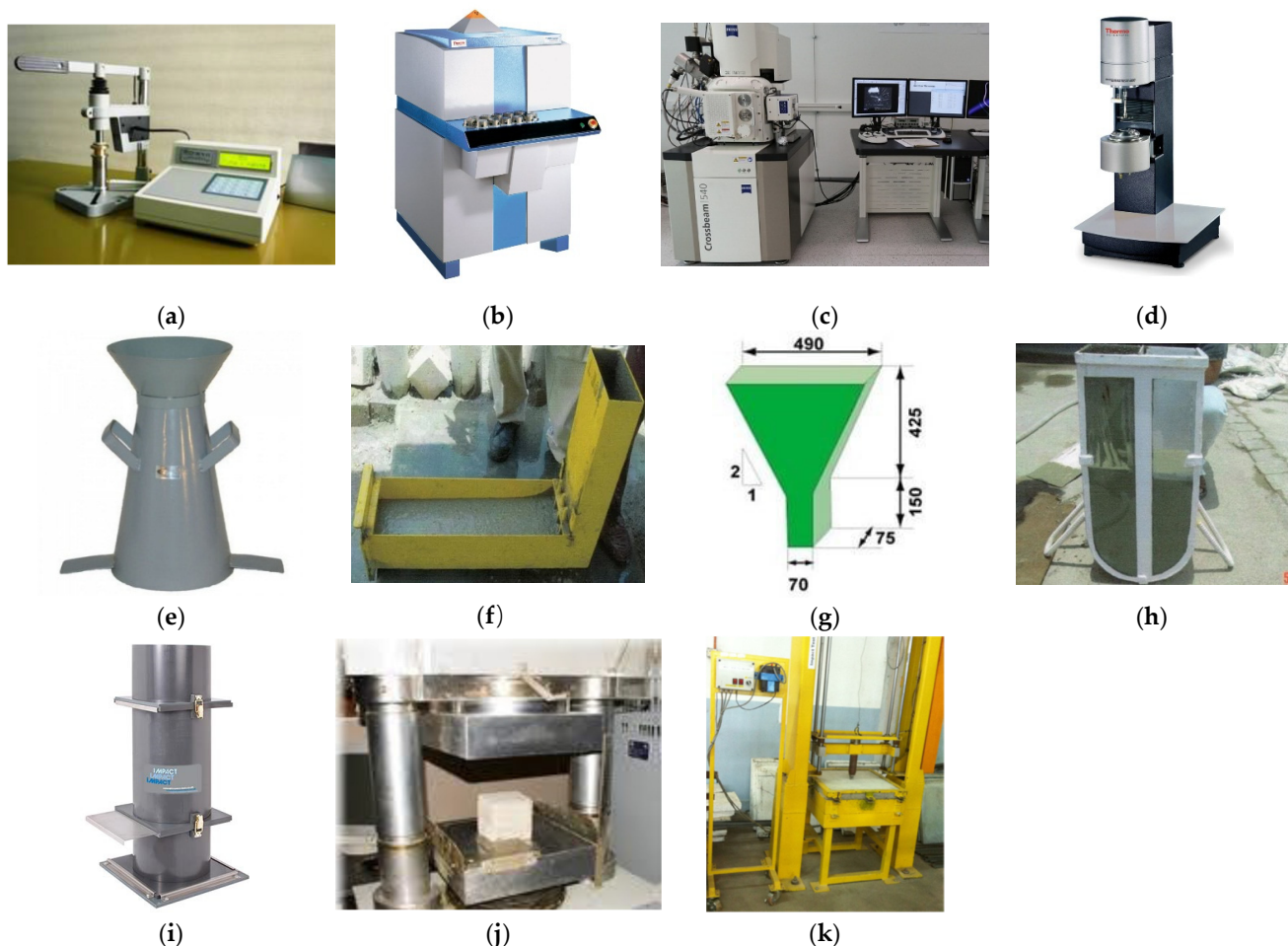

Figure 4. Equipment used: (**a**) PSH-11, (**b**) CrossBeam 1540XB; (**c**) ARL 9900 WORKSTATION; (**d**) RheoStress 600; (**e**) Abrams cone; (**f**) V-funnel; (**g**) L-box; (**h**) U-box; (**i**) Static Segregation Column Mold-HC-3666; (**j**) hydraulic press; (**k**) impact strength equipment.

According to the Russian Standard GOST 310.3-76, an Abrams cone (Figure 4e) was used to study a slump flow (in millimeters) and the velocity measure, i.e., the time (in seconds) it took for the mixture to spread up to a diameter of 500 mm. Further re-

search on self-compacting concrete mixtures was carried out according to EFNARC [45] as outlined below.

Study of the transit time of self-compacting concrete mixtures in a V-funnel in accordance with [45]. This test gives adequate results because the maximum aggregate size does not exceed 20 mm. The device consists of a 10 L stainless steel V-funnel with waterproof sliding inner surfaces. The top edge is smooth and reinforced and the outlet is equipped with a sealing valve (Figure 4f). The study of the behavior of the mixture in an L-box was used to determine the flow rates and the flow of the mixture in confined spaces. The test box consists of a concrete tank with sliding interior surfaces, three obstacles, and a test basin (Figure 4g).

A study of the behavior of the mixture via a U-box was used to measure the flowability of concrete mix in communicating vessels. The device consisted of a container, divided in the middle by a wall into two compartments, between which an opening with a sliding gate was installed (Figure 4h). Reinforcement rods with a diameter of 13.4 mm were installed on the valve with a center-to-center distance of 50 mm. This created a distance between the rods of 35 mm. The left section was filled with 20 L of concrete mixture, then the gate was lifted and the concrete began to flow into the other section. The height of the concrete mix was measured in both sections.

Static Segregation Column Mold-HC-3666 (Gilson, Columbus, OH, USA) (Figure 4i) was used to study the stratification of self-compacting concrete mix. It was also utilized to determine the potential for static separation of the mixture by measuring the fiber and aggregate content in the top and bottom of a cylindrical column. During the tests, the concrete mixture was poured into the top of the column and held for 15 min. Then the aggregate and fibers from the top and bottom of the column were collected, rinsed from the cement paste, and sieved through a 4.75 mm sieve. The segregation index (*SI*) was calculated by comparing the masses in the upper (M_u) and lower parts (M_l):

$$SI = \frac{M_l - M_u}{M_l + M_u}$$

Compressive strength was determined on cubic specimens with an edge of 150 mm using a hydraulic press (Figure 4j).

Impact strength testing was carried out using a falling impactor based on the international normative document ACI Committee 544; a slab with dimensions of $600 \times 600 \times 50$ mm was subjected to repeated impacts in one place. In this test, a striker with a weight of 10 kg fell from a height of 600 mm on the slab (Figure 4k).

3. Results and Discussion

Figure 5 demonstrates high rheological and strength characteristics of the developed composite binders.

There is an increase in strength of more than 60% at a cement substitution level of more than 40%. The obtained results of hardening and compaction of the structure are explained by the complex influence of the components of the composite binder. An active silica-containing additive and amorphous particles of ground quartz sand, as a result of a pozzolanic reaction, bind $Ca(OH)_2$, which is released during the hydration of alite into low-basic calcium silicate hydrates of the second generation. Finely ground limestone particles perform a double function: they clog the pores and form calcium hydrocarboaluminates, densifying and strengthening the structure. Crystalline particles of ground quartz sand act as centers of crystallization of new formations. This is confirmed by comparing the results obtained by other authors, for example, Tokarev et al. [46].
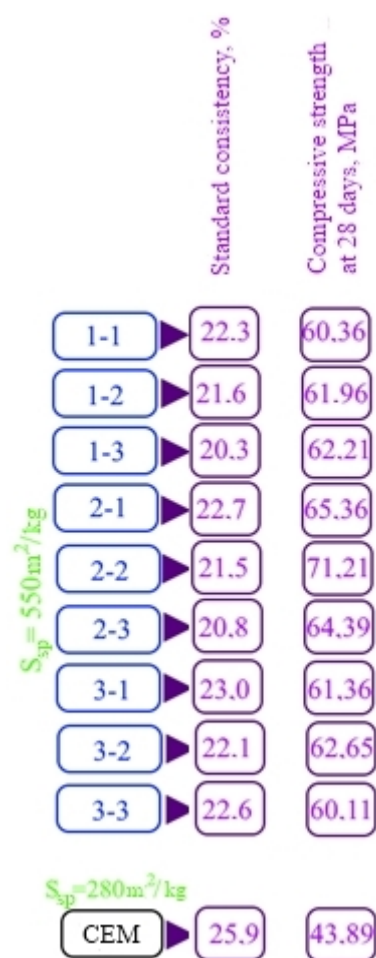
Figure 5. Rheological and strength characteristics of the developed composite binders.

Based on composite binders, self-compacting fiber-reinforced concretes have been obtained, which have the potential for use in the structures of protective structures. When reinforced with 1.6% steel fiber, they show high physical and mechanical characteristics: tensile strength—above 16.2 MPa, elastic modulus—43 GPa. The same percentage of basalt fiber reinforcement demonstrates slightly reduced indicators: tensile strength—15.8 MPa, elastic modulus—42.5 GPa. This is 15–25% higher than the results obtained by other authors in the study of various fiber-reinforced concrete [13,19].

Considering that the protective structures are mostly underground facilities, it is important to deliver the concrete mix to the work site. Accordingly, it is necessary that the workability characteristics meet the requirements for self-compacting concrete mixtures, which was achieved, according to the results shown in Figure 6. Indicators of workability of mixtures (slump flow up to 730 mm; spreading time up to a diameter of 50 cm (T_{50})—up to 3 s; flow time via a V-funnel—6 s; height difference in a U-box—up to 3 cm; ability to overcome the resistance of reinforcing bars rods in an L-box with a coefficient of up to 0.98; resistance to segregation—up to 6.3%) allow them to be classified as self-compacting concrete mixtures (corresponds to the mixture grade SF2 according to the international standards EFNARC [45]).
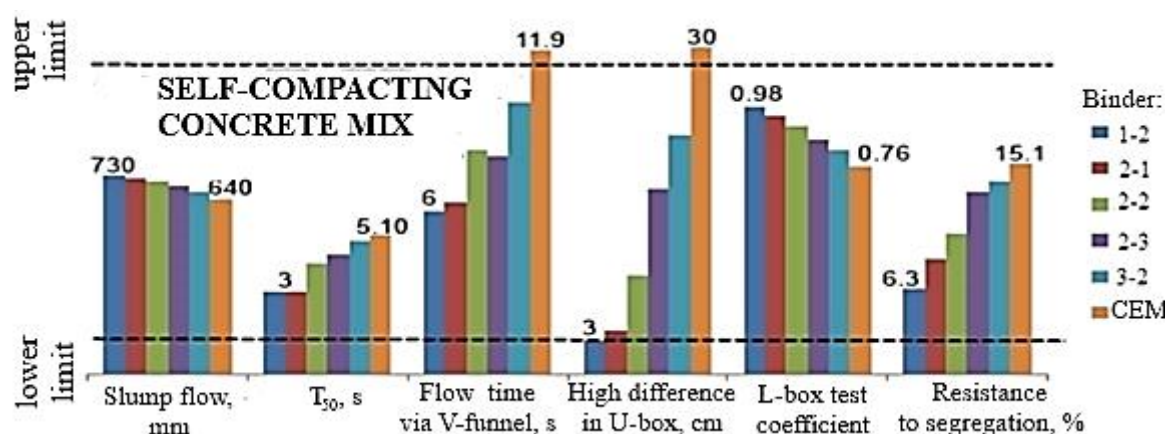
Figure 6. Achieved workability characteristics.

Despite the high workability characteristics, water separation remains at the normative level due to the use of new types of microfillers (limestone and quartz), which create a "stability framework", which has a positive effect on the homogeneity and consistency of the mixture.

An increase in the values of impact viscosity (a representative characteristic of which is the coefficient μ, which is the ratio of the number of impacts before the destruction of the sample to the number of impacts before the appearance of the first crack) by a factor of 5.5 due to the formation of the structure of fiber-reinforced concrete. Accordingly, the coefficient of dynamic hardening (CDH) increases by more than 60% due to the complex redistribution of internal stresses at the stage of hardening, as well as a decrease in the rate of cracking with a simultaneous dispersion of stresses during operation under loading. The obtained results of impact strength are 40–60% higher than the results of other authors, and by the value of the coefficient of dynamic hardening by 25–30% [47,48].

The fracture patterns of the slab specimens showed that the unreinforced plate collapsed, dividing into four parts (Figure 7a). It can be seen that the presented sample lost its structural integrity and changed its geometry, as a result of achieving the energy intensity of the impact. On the other hand, the fiber-reinforced concrete specimen (Figure 7b) was perforated as a result of repeated falling of the striker, and, accordingly, the slab did not split into pieces, remaining structurally intact and viscous; there was a large number of secondary (hair) cracks.
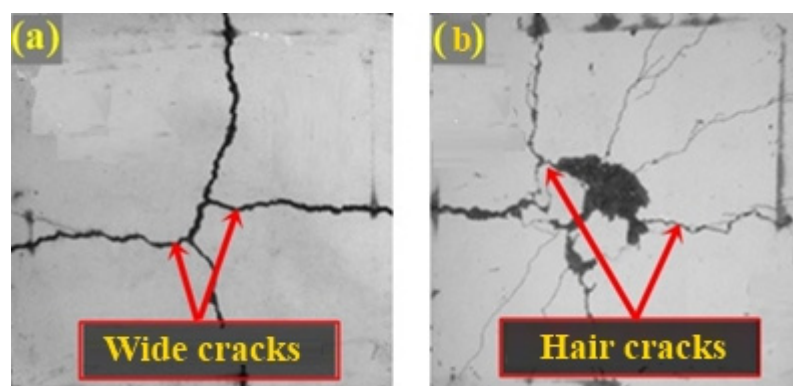

Figure 7. Patterns of destruction: unreinforced slab (**a**) and fiber-reinforced concrete (**b**).

Crack width and the number of secondary cracks appearing prior to plate failure are representative characteristics of impact viscosity. Comparing the final crack width with the initial one, the efficiency of the steel fiber is determined, which acts as a connecting "bridge" in microcracks. In particular, in the optimal composition 2-2, the crack opening

before the fracture of the specimen increased by 69% (from 1.160 to 1.876 mm), and the number of secondary cracks was more than 4 times (from 4 to 18) compared to the control specimen. SEM images of fiber-reinforced concrete show the fiber bridging effect and the compaction of the interfacial transition zone (ITZ) (Figure 8).
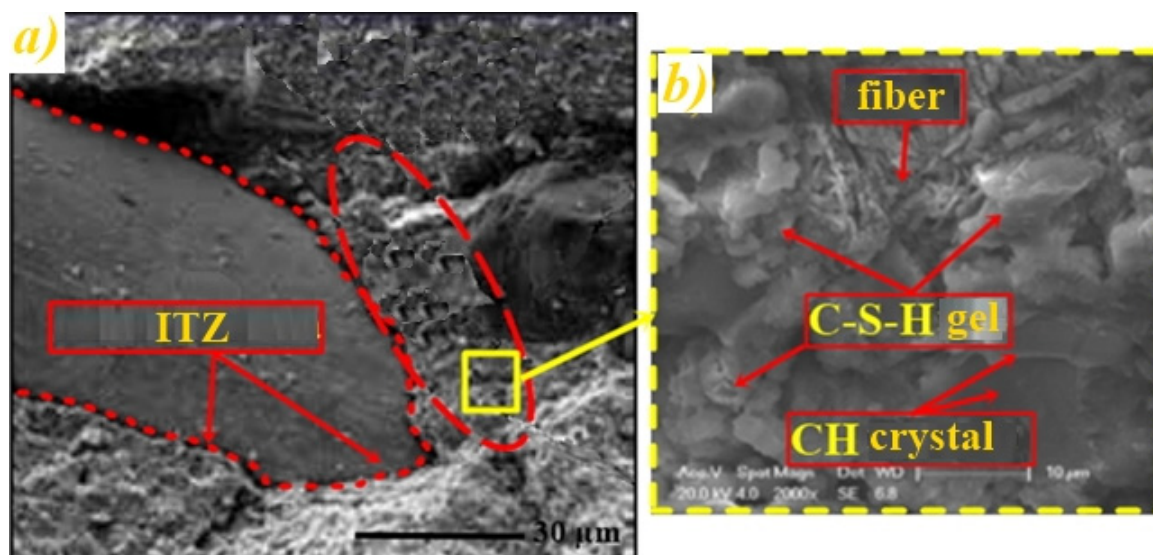

Figure 8. Morphology of synthesized composite new growths: (**a**) tight fixing of fiber in concrete; (**b**) interfacial transition zone.

Furthermore, the XRD results proved that in the developed material, in addition to amorphous silicon dioxide, there is a crystalline phase in the form of β-quartz. Both phases make it possible to control the structure formation of the developed composites (Figure 9).
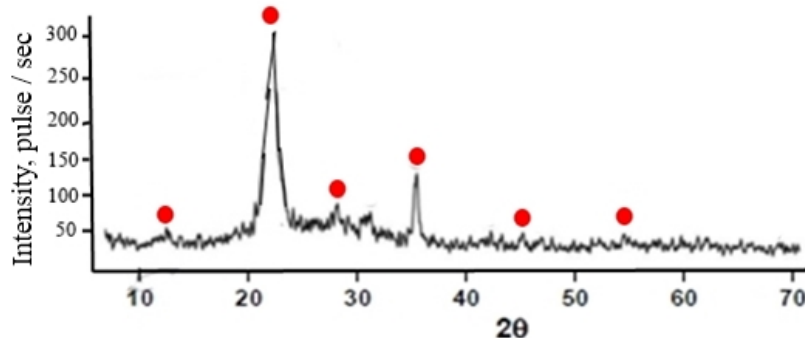

Figure 9. X-ray diffraction pattern of the specimen 2-2 with indicated reflections of β-quartz.

The study of the change in the CDH of fiber-reinforced concrete at strain rates from 30 to 110 s^{-1}, showed that sample 2-2 of the optimal composition shows a lesser dependence of deformations on loading rates (Figure 10).

In addition, in the course of calculating the coefficient of dynamic hardening according to the CEB-FIP model [29], a contradiction was established between the model and experimental results, which is especially pronounced for fiber-reinforced concrete of the optimal composition 2-2. In particular, when calculating using the CEB-FIP recommendations, the results give a higher strain rate than the results obtained experimentally; the coinciding linear dependence is traced only at an early stage, which corresponds to the rates of deformation of the transition from the elastic stage to the plastic stage (7, 11 and 15 s^{-1} for samples 2-2, 3-2 and 1-2, respectively); and at a speed of 30 s^{-1}, there is a discrepancy with the calculated data according to the CEB-FIP model. When interpolating

in the subsequent range, the calculated normative model predicts a sharper increase in CDH with the acceleration of deformation in comparison with the experimental results obtained in the work.
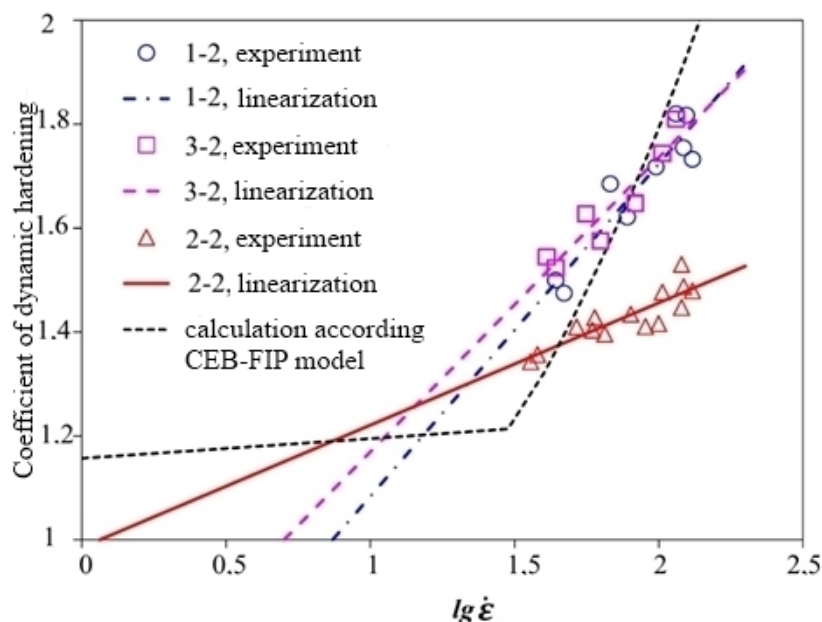

Figure 10. Comparison of the calculated and experimental values of the coefficient of dynamic hardening.

Analyzing the results obtained, the calculation Equation (1) was corrected, which makes it possible to predict the ratio of the dynamic hardening coefficient and the deformation rate of cement composites; in particular, it allows the use of the CEB-FIP recommendations for deformation rates that are lower than the deformation rate of the transition and demonstrates a linear increase in the *CDH* with a logarithmic dependence of the deformation rate higher than the deformation rate of the transition.

$$CDH = \begin{cases} (\dot{\varepsilon}/\dot{\varepsilon}_0)^{0.01} , \text{ at } \dot{\varepsilon} \leq \dot{\varepsilon}_{TR} \\ A \cdot \lg(\dot{\varepsilon}/\dot{\varepsilon}_0) + B, \text{ at } \dot{\varepsilon} > \dot{\varepsilon}_{TR} \end{cases} \tag{1}$$

where $\dot{\varepsilon}_0 = 30 \times 10^{-6}$ s^{-1}, $\dot{\varepsilon}_{TR}$ are the deformation rates of the transition, *A* and *B* are the constants established experimentally. The values of the coefficients are: *A* (0.7394; 0.9872 and 0.1209), *B* (−2.9830; −0.8409 and −2.1270) and $\dot{\varepsilon}_{TR}$ (15, 7 and 11) for samples 1-2, 2-2 and 3-2, respectively. The results of the calculated values according to the proposed formula show good reliability (R^2 = 0.9548). In this case, the error of the model (*p*-value) amounts to 0.0015.

Thus, the results obtained confirm the possibility of obtaining self-compacting fiber concretes capable of providing improved physical and mechanical properties and performances as a result of using the composite binder consisting of an active silica-containing additive, a complex of micro-fillers, as well as steel or basalt fiber. It was found that fiber-reinforced cement composites, with a small number of defects, due to which they are high-density and relatively homogeneous, having high adhesion between the composite matrix, fine aggregate and fiber, characterized by an increased ratio between tensile and compressive strengths, have good impact viscosity.

The factor of impact viscosity increased by 5.5 times due to the formation of the structure of the composite matrix and absorption of the impact energy by the fiber, as well as the increased characteristics of self-sealing, prove the effectiveness of using the developed materials for the construction of protective underground structures of complex configuration.

4. Conclusions

The development and research of nine high-performance concrete mixtures made it possible to achieve improved physical and mechanical properties and performances of the fiber-reinforced concrete, which allows them to be used for protective structures. The main conclusions of the current research can be summarized by the followings:

- The processes of structure formation in multicomponent polymineral hardening systems based on composite binders using nature-like technologies were examined through experimental tests and supplemented when creating building materials for operation in extreme conditions.
- A wide range of fiber-reinforced concretes based on composite binder has been prepared, with increased characteristics of impact strength. The influence of the manufacturing technology of cement composites on the coefficient of dynamic hardening has been established, while the growth of these indicators attributed a denser interfacial transition zone between the cement paste, aggregate, and fiber as a result of improving the homogeneity of the concrete mixture and controlling the consistency.
- The dependence of the viscosity of mixtures on the type of composite binder has been studied. The workability indices of the mixes make it possible to classify them as self-compacting concrete mixes (grade SF2 by the value of slump flow). The high workability of fiber-reinforced concrete mixtures makes it possible to use them for the construction of objects of complex configuration in terms of plan, including underground civil defense facilities.
- An increase in the values of the impact strength coefficient up to 5.5 times, the dynamic hardening coefficient by almost 70% as a result of a directionally synthesized binder matrix, as well as absorption of impact energy by fiber, was revealed. The mechanical changes should be attributed to the mechanical properties of the binder and the ITZ.

Author Contributions: Conceptualization, R.F.; methodology, M.A.; software, S.K.; validation, A.K.; resources, R.F.; writing—original draft preparation, R.F., M.A., S.K. and A.K.; visualization, R.F.; supervision, M.A. All authors have read and agreed to the published version of the manuscript.

Institutional Review Board Statement: Not applicable.

Informed Consent Statement: Not applicable.

Data Availability Statement: Not applicable.

Conflicts of Interest: The authors declare no conflict of interest.

References

1. Amran, M.; Fediuk, R.; Vatin, N.; Lee, Y.H.; Murali, G.; Ozbakkaloglu, T.; Klyuev, S.; Alabduljabber, H. Fibre-Reinforced Foamed Concretes: A Review. *Materials* **2020**, *13*, 4323. [CrossRef]
2. Amran, Y.M.; Alyousef, R.; Alabduljabbar, H.; Khudhair, M.; Hejazi, F.; Alaskar, A.; Alrshoudi, F.; Siddika, A. Performance Properties of Structural Fibred-Foamed Concrete. *Results Eng.* **2020**, *5*, 100092. [CrossRef]
3. Murali, G.; Abid, S.; Amran, M.; Fediuk, R.; Vatin, N.; Karelina, M. Combined Effect of Multi-Walled Carbon Nanotubes, Steel Fibre and Glass Fibre Mesh on Novel Two-Stage Expanded Clay Aggregate Concrete against Impact Loading. *Crystals* **2021**, *11*, 720. [CrossRef]
4. Murali, G.; Abid, S.R.; Karthikeyan, K.; Haridharan, M.; Amran, M.; Siva, A. Low-Velocity Impact Response of Novel Prepacked Expanded Clay Aggregate Fibrous Concrete Produced with Carbon Nano Tube, Glass Fiber Mesh and Steel Fiber. *Constr. Build. Mater.* **2021**, *284*, 122749. [CrossRef]
5. Rossi, P.; Arca, A.; Parant, E.; Fakhri, P. Bending and Compressive Behaviours of a New Cement Composite. *Cem. Concr. Res.* **2005**, *35*, 27–33. [CrossRef]
6. Murphy, F.; Pavia, S.; Walker, R. An assessment of the physical properties of lime-hemp concrete. In Proceedings of the Bridge and Concrete Research, Cork, Ireland, 2–3 September 2010; pp. 431–438.

7.   Al-Nini, A.; Nikbakht, E.; Syamsir, A.; Shafiq, N.; Mohammed, B.S.; Al-Fakih, A.; Al-Nini, W.; Amran, Y.H.M. Flexural Behavior of Double-Skin Steel Tube Beams Filled with Fiber-Reinforced Cementitious Composite and Strengthened with CFRP Sheets. *Materials* **2020**, *13*, 3064. [CrossRef]

8.   Adamczyk, W.P.; Gorski, M.; Ostrowski, Z.; Bialecki, R.; Kruczek, G.; Przybyła, G.; Krzywon, R.; Bialozor, R. Application of Numerical Procedure for Thermal Diagnostics of the Delamination of Strengthening Material at Concrete Construction. *Int. J. Numer. Methods Heat Fluid Flow* **2019**, *30*, 2655–2668. [CrossRef]

9.   Fediuk, R.S.; Ibragimov, R.A.; Lesovik, V.S.; Pak, A.A.; Krylov, V.V.; Poleschuk, M.M.; Stoyushko, N.Y.; Gladkova, N.A. Processing Equipment for Grinding of Building Powders. *IOP Conf. Ser. Mater. Sci. Eng.* **2018**, *327*, 042029. [CrossRef]

10. Lesovik, V.S. The Reducing Effect of Argon in the Plasma Treatment of High-Melting Nonmetallic Materials (A Review). *Glas. Ceram.* **2001**, *58*, 362–364.

11. Chernysheva, N.; Lesovik, V.; Fediuk, R.; Vatin, N. Improvement of Performances of the Gypsum-Cement Fiber Reinforced Composite (GCFRC). *Materials* **2020**, *13*, 3847. [CrossRef]

12. Szeląg, M. Properties of Cracking Patterns of Multi-Walled Carbon Nanotube-Reinforced Cement Matrix. *Materials* **2019**, *12*, 2942. [CrossRef] [PubMed]

13. Rucka, M.; Wojtczak, E.; Knak, M.; Kurpińska, M. Characterization of Fracture Process in Polyolefin Fibre-Reinforced Concrete Using Ultrasonic Waves and Digital Image Correlation. *Constr. Build. Mater.* **2021**, *280*, 122522. [CrossRef]

14. Lesovik, V.; Voronov, V.; Glagolev, E.; Fediuk, R.; Alaskhanov, A.; Amran, Y.M.; Murali, G.; Baranov, A. Improving the Behaviors of Foam Concrete Through the Use of Composite Binder. *J. Build. Eng.* **2020**, *31*, 101414. [CrossRef]

15. Khan, M.; Cao, M.; Xie, C.; Ali, M. Hybrid Fiber Concrete with Different Basalt Fiber Length and Content. *Struct. Concr.* **2021**, 51678111. [CrossRef]

16. Fediuk, R.S.; Lesovik, V.S.; Mochalov, A.V.; Otsokov, K.A.; Lashina, I.V.; Timokhin, R.A. Composite Binders for Concrete of Protective Structures. *Mag. Civ. Eng.* **2018**, *82*, 208–218. [CrossRef]

17. Amran, Y.H.M. Influence of Structural Parameters on the Properties of Fibred-Foamed Concrete. *Innov. Infrastruct. Solut.* **2020**, *5*, 16. [CrossRef]

18. Khan, M.; Cao, M.; Xie, C.; Ali, M. Efficiency of Basalt Fiber Length and Content on Mechanical and Microstructural Properties of Hybrid Fiber Concrete. *Fatigue Fract. Eng. Mater. Struct.* **2021**, *44*, 2135–2152. [CrossRef]

19. Khan, M.; Cao, M. Effect of Hybrid Basalt Fibre Length and Content on Properties Of Cementitious Composites. *Mag. Concr. Res.* **2021**, *73*, 487–498. [CrossRef]

20. Siddika, A.; Al Mamun, A.; Alyousef, R.; Amran, Y.M. Strengthening of Reinforced Concrete Beams by Using Fiber-Reinforced Polymer Composites: A review. *J. Build. Eng.* **2019**, *25*, 100798. [CrossRef]

21. Khan, M.; Cao, M.; Hussain, A.; Chu, S. Effect of Silica-Fume Content on Performance of Caco3 Whisker and Basalt Fiber at Matrix Interface in Cement-Based Composites. *Constr. Build. Mater.* **2021**, *300*, 124046. [CrossRef]

22. Haridharan, M.; Matheswaran, S.; Murali, G.; Abid, S.R.; Fediuk, R.; Amran, Y.M.; Abdelgader, H.S. Impact Response of Two-Layered Grouted Aggregate Fibrous Concrete Composite under Falling Mass Impact. *Constr. Build. Mater.* **2020**, *263*, 120628. [CrossRef]

23. Murali, G.; Abid, S.R.; Amran, Y.M.; Abdelgader, H.S.; Fediuk, R.; Susrutha, A.; Poonguzhali, K. Impact Performance of Novel Multi-Layered Prepacked Aggregate Fibrous Composites under Compression and Bending. *Structures* **2020**, *28*, 1502–1515. [CrossRef]

24. Abid, S.R.; Murali, G.; Amran, M.; Vatin, N.; Fediuk, R.; Karelina, M. Evaluation of Mode II Fracture Toughness of Hybrid Fibrous Geopolymer Composites. *Materials* **2021**, *14*, 349. [CrossRef]

25. Murali, G.; Abid, S.R.; Abdelgader, H.S.; Amran, Y.H.M.; Shekarchi, M.; Wilde, K. Repeated Projectile Impact Tests on Multi-Layered Fibrous Cementitious Composites. *Int. J. Civ. Eng.* **2021**, *19*, 635–651. [CrossRef]

26. Kalinichev, A.; Wang, J.; Kirkpatrick, R.J. Molecular Dynamics Modeling of the Structure, Dynamics and Energetics of Mineral–Water Interfaces: Application to Cement Materials. *Cem. Concr. Res.* **2007**, *37*, 337–347. [CrossRef]

27. Yoo, D.-Y.; Banthia, N.; Yoon, Y.-S. Flexural Behavior of Ultra-High-Performance Fiber-Reinforced Concrete Beams Reinforced with GFRP and Steel Rebars. *Eng. Struct.* **2016**, *111*, 246–262. [CrossRef]

28. Ranjbar, N.; Zhang, M. Fiber-Reinforced Geopolymer Composites: A Review. *Cem. Concr. Compos.* **2020**, *107*, 103498. [CrossRef]

29. Favre, R.; Charif, H. Basic model and simplified calculations of deformations according to the CEB-FIP model code 1990. *Struct. J.* **1994**, *91*, 169–177.

30. Salaimanimagudam, M.P.; Murali, G.; Vardhan, C.M.V.; Amran, M.; Vatin, N.; Fediuk, R.; Vasilev, Y. Impact Response of Preplaced Aggregate Fibrous Concrete Hammerhead Pier Beam Designed with Topology Optimization. *Crystals* **2021**, *11*, 147. [CrossRef]

31. Murali, G.; Amran, M.; Fediuk, R.; Vatin, N.; Raman, S.N.; Maithreyi, G.; Sumathi, A. Structural Behavior of Fibrous-Ferrocement Panel Subjected to Flexural and Impact Loads. *Materials* **2020**, *13*, 5648. [CrossRef] [PubMed]

32. Temuujin, J.; Minjigmaa, A.; Davaabal, B.; Bayarzul, U.; Ankhtuya, A.; Jadambaa, T.; MacKenzie, K. Utilization of Radioactive High-Calcium Mongolian Flyash for the Preparation of Alkali-Activated Geopolymers for Safe Use as Construction Materials. *Ceram. Int.* **2014**, *40*, 16475–16483. [CrossRef]

33. Amran, M.; Debbarma, S.; Ozbakkaloglu, T. Fly ash-based eco-friendly geopolymer concrete: A critical review of the long-term durability properties. *Constr. Build. Mater.* **2021**, *270*, 121857. [CrossRef]

34. Murtazaiev, S.-A.Y.; Lesovik, V.S.; Bataiev, D.K.-S.; Chernysheva, N.V.; Saidumov, M.S. Fine-Grainedcellular Concrete Creep Analysis Technique with Consideration Forcarbonation. *Mod. Appl. Sci.* **2015**, *9*, 233. [CrossRef]

35. Jaishankar, P.; Murali, G.; Salaimanimagudam, M.P.; Amran, Y.H.M.; Fediuk, R.; Karthikeyan, K. Study of Topology Optimized Hammerhead Pier Beam Made with Novel Preplaced Aggregate Fibrous Concrete. *Period. Polytech. Civ. Eng.* **2020**, *65*, 287–298. [CrossRef]

36. Semenov, P.; Uzunian, A.; Davidenko, A.; Derevschikov, A.; Goncharenko, Y.; Kachanov, V.; Khodyrev, V.; Meschanin, A.; Minaev, N.; Mochalov, V.; et al. First Study of Radiation Hardness of Lead Tungstate Crystals at Low Temperatures. *Nucl. Instrum. Methods Phys. Res. Sect. A Accel. Spectrometers Detect. Assoc. Equip.* **2007**, *582*, 575–580. [CrossRef]

37. Fediuk, R.S.; Yevdokimova, Y.G.; Smoliakov, A.K.; Stoyushko, N.Y.; Lesovik, V.S. Use of Geonics Scientific Positions for Designing of Building Composites for Protective (Fortification) Structures. *IOP Conf. Ser. Mater. Sci. Eng.* **2017**, *221*, 012011. [CrossRef]

38. Fediuk, R.S. Mechanical Activation of Construction Binder Materials by Various Mills. *IOP Conf. Ser. Mater. Sci. Eng.* **2016**, *125*, 012019. [CrossRef]

39. Volodchenko, A.A.; Lesovik, V.S.; Volodchenko, A.N.; Glagolev, E.S.; Zagorodnjuk, L.H.; Pukharenko, Y.V. Composite Performance Improvement Based on Non-Conventional Natural and Technogenic Raw Materials. *Int. J. Pharm. Technol.* **2016**, *8*, 18856–18867.

40. Fediuk, R. High-Strength Fibrous Concrete of Russian Far East Natural Materials. *IOP Conf. Ser. Mater. Sci. Eng.* **2016**, *116*, 012020. [CrossRef]

41. Elistratkin, M.; Kozhuhova, M. Analysis of the Factors of Increasing the Strength of the Non-Autoclave Aerated Concrete. *Constr. Mater. Prod.* **2020**, *1*, 59–68. [CrossRef]

42. Klyuyev, S.; Guryanov, Y. External Reinforcing of Fiber Concrete Constructions by Carbon Fiber Tapes. *Mag. Civ. Eng.* **2013**, *36*, 21–26. [CrossRef]

43. Ramakrishnan, K.; Depak, S.; Hariharan, K.; Abid, S.R.; Murali, G.; Cecchin, D.; Fediuk, R.; Amran, Y.M.; Abdelgader, H.S.; Khatib, J.M. Standard and Modified Falling Mass Impact Tests on Preplaced Aggregate Fibrous Concrete and Slurry Infiltrated Fibrous Concrete. *Constr. Build. Mater.* **2021**, *298*, 123857. [CrossRef]

44. Sanjuán, M.A.; Argiz, C. La Nueva Norma Europea de Especificaciones de Cementos Comunes UNE-EN 197-1:2011. *Mater. Constr.* **2012**, *62*, 425–430. [CrossRef]

45. EFNARC. *Specification and Guidelines for Self-Compacting Concrete*; EFNARC: Farnham, UK, 2002; ISBN 0-9539733-4-4.

46. Tokarev, Y.; Yakovlev, G.; Saidova, Z.; Grakhov, V.; Buryanov, A.; Elrefai, A.E.M.M. A Study on Mechanical Properties and Structure of Anhydrite Binder Modified by Ultra-Dispersed Siltstone. *Eng. Struct. Technol.* **2020**, *11*, 78–86. [CrossRef]

47. Murali, G.; Ramprasad, K. A Feasibility of Enhancing the Impact Strength of Novel Layered Two Stage Fibrous Concrete Slabs. *Eng. Struct.* **2018**, *175*, 41–49. [CrossRef]

48. de Azevedo, A.R.; Marvila, M.T.; Tayeh, B.A.; Cecchin, D.; Pereira, A.C.; Monteiro, S.N. Technological Performance of Açaí Natural Fibre Reinforced Cement-Based Mortars. *J. Build. Eng.* **2021**, *33*, 101675. [CrossRef]